Biochimica et Biophysica Acta 903 (1987) 319–332
Elsevier

BBA 73692

Co-solubility in binary phospholipid crystals

Douglas L. Dorset and Andrew K. Massalski

Electron Diffraction Department, Medical Foundation of Buffalo, Inc., Buffalo, NY (U.S.A.)

(Received 6 April 1987)

Key words: Phase diagram; Differential scanning calorimetry; Electron diffraction; Epitaxial crystallization

Crystalline binary solid solutions of phosphatidylethanolamines are obtained when various fractions of compounds with different chain lengths are dissolved in chloroform and allowed to evaporate to dryness. Phase diagrams and electron diffraction measurements on chain mixtures with a difference of two or four methylene groups indicate that solubility is continuous, although non-ideal. Average molecular volume appears to increase according to Vegard's rule although deviations are noted. These deviations are similar to those observed for binary paraffin solids. Substitution of ether-links for ester-links in one component does not alter solubility behavior. In general the rules of solid solution formation appear to conform to those originally proposed by Kitaigorodskii ((1961) Organic Chemical Crystallography, pp. 231–240, Consultants Bureau, New York).

Introduction

The validity of structural models for phospholipid packing in biomembranes depends on at least two assumptions. One is that the crystal structure of a minimally solvated phosphatide represents a molecular conformation similar to that found in an excess of water. This assumption often appears to be justified by a comparison of a small number of three-dimensional crystal structures [1–5] to e.g. neutron diffraction studies of hydrated phospholipid multilayers in which the molecules are selectively deuterated to allow localization of specific residues [6–8].

A second assumption is that the molecular packing in the polydisperse mixture found in natural biomembranes is similar to that found for monodisperse bilayers. This can be supported by a comparison of one-dimensional electron density maps from X-ray diffraction analyses from e.g. the myelin sheath [9–13] to those from single component bilayers [14–17].

The existence of polydisperse bilayers in nature is also known to introduce an additional complication to membrane structure, i.e., as suggested by numerous studies of model binary phospholipid systems in the presence of water, a membrane can contain adjacent lateral microareas with varying fluidity, a phenomenon which is dependent on the phase behavior of local lipid composition. Co-solubility of two phospholipids can depend on a number of factors such as relative chain length [18–22], chain unsaturation [20–21], headgroup species [22], and, possibly, degree of solvation [23–26]. Although considerable data on the phase behavior of quasi-binary phospholipid mixtures in the presence of excess water have been published, comparably little structural information is available to interpret the phase diagram and to resolve conflicting claims of miscibility or fractionation of a particular binary mixture.

It is most desirable to explain the phase behav-

Correspondence: D.L. Dorset, Electron Diffraction Department, Medical Foundation of Buffalo, Inc., 73 High Street, Buffalo, NY 14203, U.S.A.

ior of such mixtures in terms of molecular packing, e.g. according to the rules proposed by Kitaigorodskii [27], for the formation of continuous solid solutions. Achievement of this goal via X-ray crystal structures may be very difficult for, as shown by Albon [28], the mere presence of a chain length mixture can severely impede crystal growth. A more likely approach may be to use electron diffraction techniques on more readily available microcrystals since preliminary studies on epitaxially crystallized paraffins [29,30] and cholesteryl esters [31] have been particularly successful in correlating co-solubility and fractionation to the crystal structures and molecular volumes of the pure components.

This paper describes an initial study of phosphatidylethanolamine mixtures based on electron diffraction and high resolution electron microscopy of epitaxially nucleated crystals. The phospholipid class is chosen since it is only hydrated with difficulty [32] (and thus anhydrous crystals are independent of possible vacuum-drying effects in the electron microscope) and because the crystal structures and multilamellar packings of racemic and chiral homologs have been described in the literature [1,2,8,33–35].

Materials and Methods

Crystallization

Chiral phosphatidylethanolamines in a homologous series including 1,2-dilauroyl-*sn*-glycerophosphoethanolamine (DLPE), 1,2-dimyristoyl-*sn*-glycerophosphoethanolamine (DMPE), and 1,2-dipalmitoyl-*sn*-glycerophosphoethanolamine (DPPE), as well as the ether linked 1,2-dihexadecyl-*sn*-glycerophosphoethanolamine (DHPE), were purchased from Calbiochem-Behring (La Jolla, CA) and were used without further purification. The racemic lipid 1,2-dipalmitoyl-*rac*-glycerophosphoethanolamine (DL-DPPE) was obtained from Sigma Chemical (St. Louis, MO). The essential purity of these samples is established from the measured lamellar spacings in electron diffraction patterns from epitaxially crystallized samples [34] and the match of diffraction intensity data with model data based on a reasonable crystal structure adjusted for the proper chain length [33,34]. The absence of a split endotherm peak for the crystalline to smectic transition in DSC scans may also indicate the lack of significant amounts of lysophosphatide contaminant [36] if an analogy exists between aqueous dispersions and anhydrous samples of the lipids, as is indicted by our observations on degraded samples.

Samples of the pure materials or preweighed binary mixtures were solubilized in warm $CHCl_3$. Epitaxial crystallization on naphthalene or benzoic acid was carried out using the procedure of Wittmann et al. [37]. Briefly, after cleaving a mica sheet, some chloroform solution of the lipid or the binary mixture is evaporated on the clean surface and carbon film-covered electron microscope grids are placed over areas where thin crystalline layers remain. Larger amounts of either naphthalene or benzoic acid are sprinkled around the grids and the other half of the mica sheet placed over this physical mixture to form a sandwich. The lamellar sandwich is moved along a temperature gradient until the nucleating substrate melts to dissolve the phospholipid. Upon cooling, a eutectic is formed and the epitaxial nucleation of the phospholipid is directed by the aromatic compound via lattice matching with the polymethylene chains [37]. Unlike crystallization from solution, this places the long unit cell axis parallel to a major crystal face.

For differential scanning calorimetry, chloroform solutions of the pure lipid or binary mixtures are evaporated in an aluminum crucible with a stream of dichlorodifluoromethane ('Dust-off', Polysciences Inc., Warrington, PA) to leave the mixed solids. Residual traces of solvent are removed under vacuum (approx. 10^{-5} torr) by allowing the specimens to sit overnight in a vacuum coater unit.

Electron diffraction and low-dose electron microscopy

Selected area diffraction experiments were carried out at 100 kV with a JEOL JEM-100B electron microscope, taking usual precautions [38] that minimal exposure of the specimen to the electron beam was made to eliminate significant radiation damage to the crystalline specimen. The camera length of the diffraction experiment was calibrated with a gold Debye-Scherrer diagram photographed at the same lens settings. When necessary, heating experiments in the electron microscope

were possible with a GATAN 626 specimen holder which is capable of holding temperatures in the range $-170\,^{\circ}C$ to $+150\,^{\circ}C$ within a fraction of a degree variation.

Low dose electron microscopy of the crystalline samples was carried out at a 20000 × working magnification using beam currents similar to those used for electron diffraction. Images were photographed on the same Kodak DEF-5 X-ray film used for electron diffraction experiments, which was developed for 5 min in Kodak Industrex developer to give a film grain size of approx. 14 μm. This would allow a direct resolution of 7 Å, and is compared to the 16 Å resolution often observed in optical transforms. (Thus the resolution limit is set by the phase contrast transfer function of an underfocussed objective lens.) For low-dose microscopy, a procedure described by Fryer and Dorset [39] is used. That is, the microscope is first corrected for objective lens astigmatism at very high magnification (e.g. 100000 ×) and then returned to the working magnification and low beam current settings. The specimen is then scanned in diffraction mode until a diffraction pattern with suitable resolution is found. Immediately the specimen is translated to a nearby area to allow focussing on an edge. After translating back to the original point in diffraction mode the beam is swept away from the area with deliberately misaligned 'dark field' controls in the deflector system. After a film is translated into position and the fluorescent screen is raised, the illumination is swept back to the specimen with a aligned 'bright field' setting for a short exposure. After a second beam deflection, the objective lens can be further underfocussed for photography of a focal series (usually three micrographs) and, after the focal series is photographed, the integrity of the sample is checked by observation of the electron diffraction pattern. Usually crystalline areas are directly observable on the photographic negative but the image resolution may be determined from an optical diffraction pattern obtained with an optical bench (e.g. Polaron Instruments, Hatfield, PA).

Differential scanning calorimetry

Qualitative differential scanning calorimetry measurements were made on the specimens (after the $CHCl_3$ solutions were evaporated, dried and sealed in aluminum crucibles) with a Mettler FP800 thermosystem. The scan rate was generally 5 K/min. Given the monotropic nature of the phase transitions [40], only heating scans were done and the specimens were then discarded. Phase diagrams were drawn from the DSC scans using the onset and return temperatures of two major endotherms (as discussed below) to define the limits of two-phase regions. (With the recent aquisition of a Mettler TA-3300 calorimeter in this laboratory, the transition temperatures for pure phospholipids were redetermined for comparison to results obtained on the FP800 system to establish that they are correct.)

Results

Phase behavior of pure phosphatidylethanolamines

DSC scans form pure phosphatidylethanola-

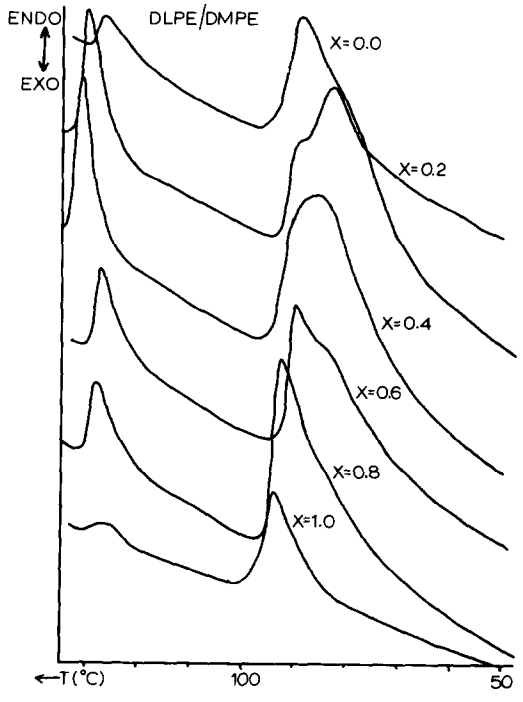

Fig. 1. DSC scans of binary mixtures (mole fraction DMPE = *X*) of 1,2-dilauroyl-*sn*-glycerophosphoethanolamine (DLPE) and 1,2-dimyristoyl-*sn*-glycerophosphoethanolamine (DMPE). The largest endothermic peak denotes a crystalline to smectic transition which is enantiotropic and the smaller one is a monotropic transition from the smectic to another liquid crystalline state [49]. (In this figure the peak heights in individual scans are not normalized to a constant molar amount of lipid.)

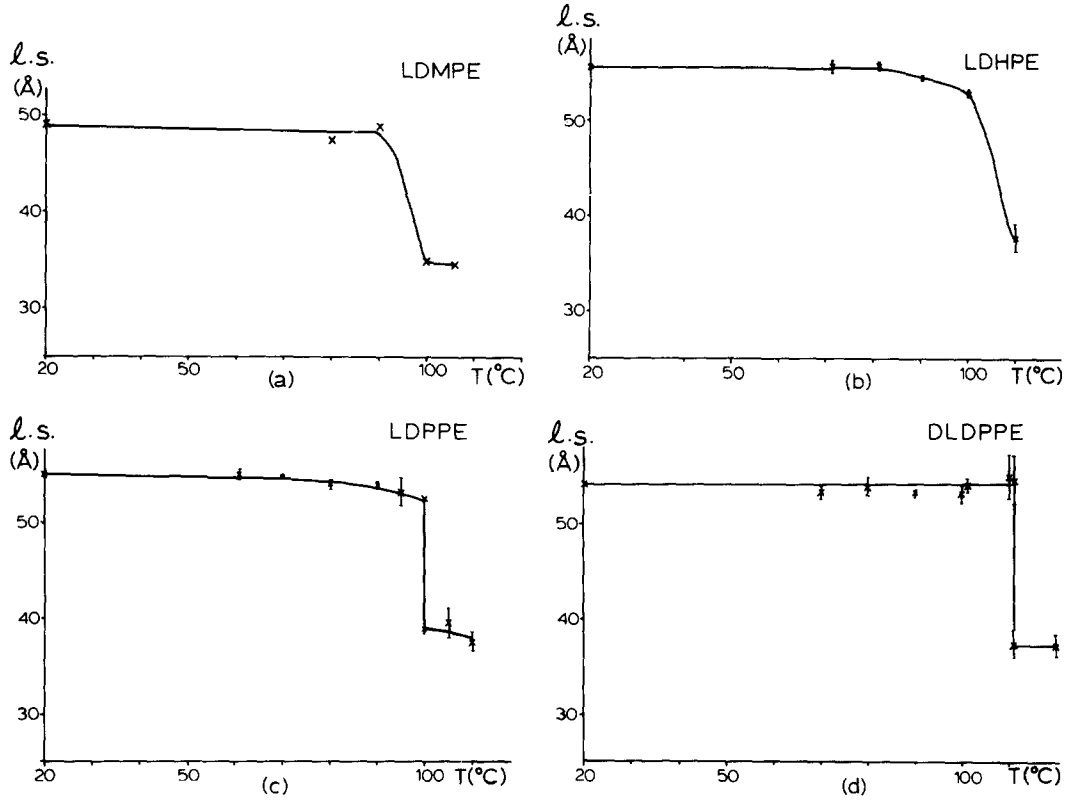

Fig. 2. Plots of lamellar spacings from electron diffraction patterns for heated samples of anhydrous 1,2-diradylphosphatidylethanolamines epitaxially crystallized on naphthalene: (a) *sn*-1,2-dimyristoyl (DMPE), (b) *sn*-1,2-dihexadecyl (DHPE), (c) *sn*-1,2-dipalmitoyl (DPPE), (d) *rac*-1,2-di-palmitoyl (DL-DPPE).

mines (Fig. 1) are similar to those published earlier for unhydrated specimens [40]. Comparison to a plot of lamellar spacing vs. temperature (Fig. 2) for these compounds reveals that the sharp changes of lamellar specing, in most cases, approximately corresponds to the return temperature of the largest DSC peak. As seen in Table I, which reviews the transition temperatures obtained from electron and/or previously published X-ray diffraction data, the phase change from the crystalline to smectic liquid crystalline state occurs at somewhat higher temperature for racemic mixtures than for the optically active material. The crystal structures for the chiral and racemic compounds are nevertheless similar, as described elsewhere [34,35]. Although the structure is not quantitatively verified by structure analysis with the diffraction intensity data, the transition to a lamellar spacing with a much shorter spacing, which was also noted in an earlier X-ray studies [40], could possibly be due to an interdigitated chain structure similar to the one described for phosphatidylcholines [41–43].

Representative electron diffraction patterns

Fig. 3. Electron diffraction patterns from epitaxially crystallized phosphatidylethanolamines. The row of closely spaced spots on the equator represents the lamellar repeat while the meridional spots (or rings) denote the side-to-side chain packing (see Ref. 34). Pure 1,2-dipalmitoyl-*sn*-glycerophosphoethanolamine heated in the electron microscope (a) 18 °C, (b) 90 °C, both showing crystalline diffraction patterns (with lamellar spacings, respectively, 55.0 Å and 54.0 Å. Pure DPPE heated in the electron microscope (c) 105 °C with a pattern from the smectic mesomorph (lamellar spacing = 39.6 Å). Binary solid solutions: (d) DMPE/DPPE 1:3 with a crystalline molecular packing, (e) DMPE/DHPE 1:4 with a smectic mesophase packing (lamellar spacing = 32.4 Å) and (f) DLPE/DPPE 1:3 with a crystalline molecular packing. (See also Fig. 6).

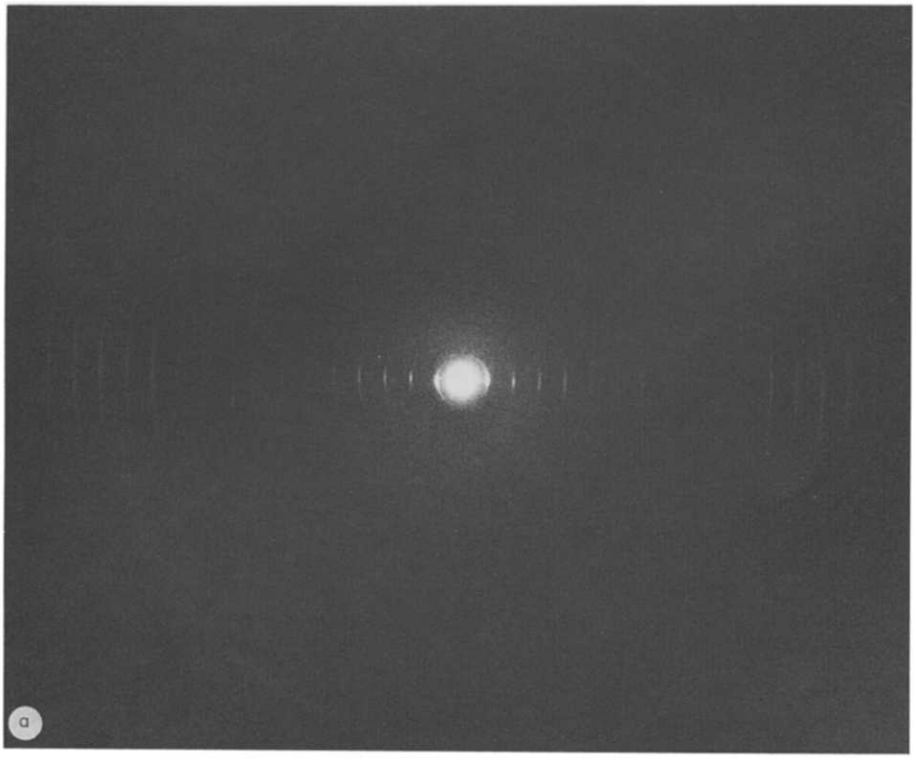
a

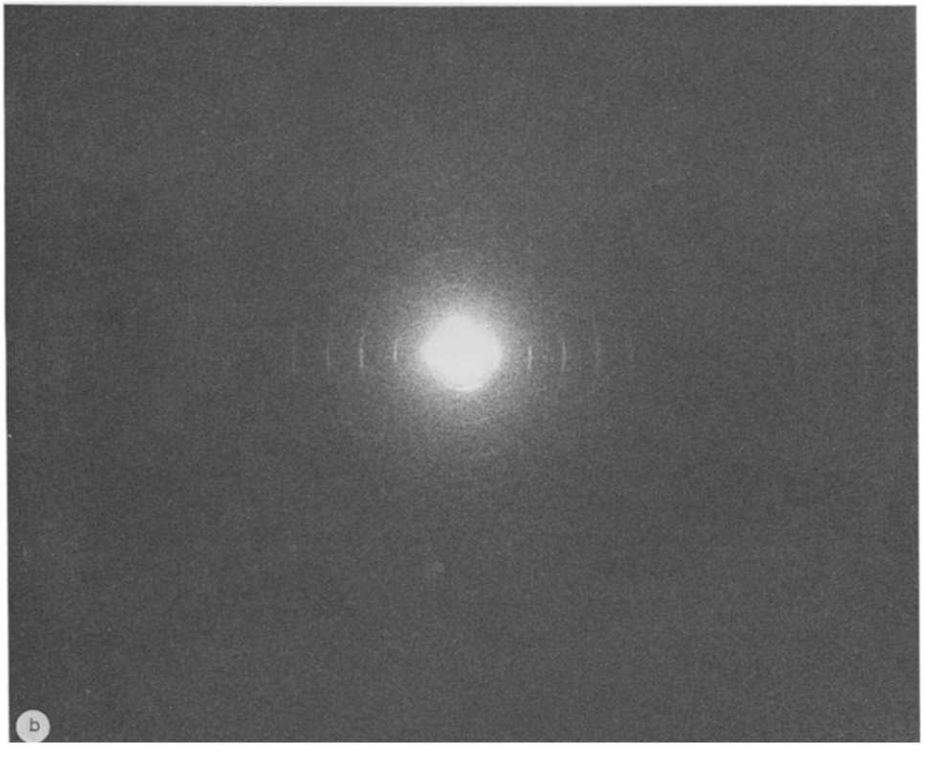
b

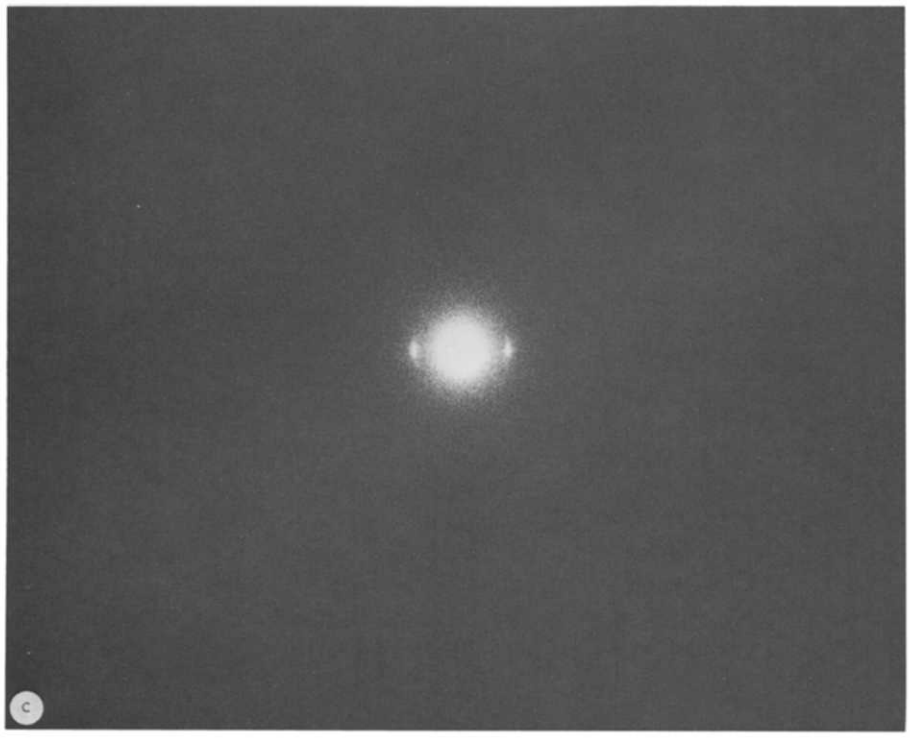

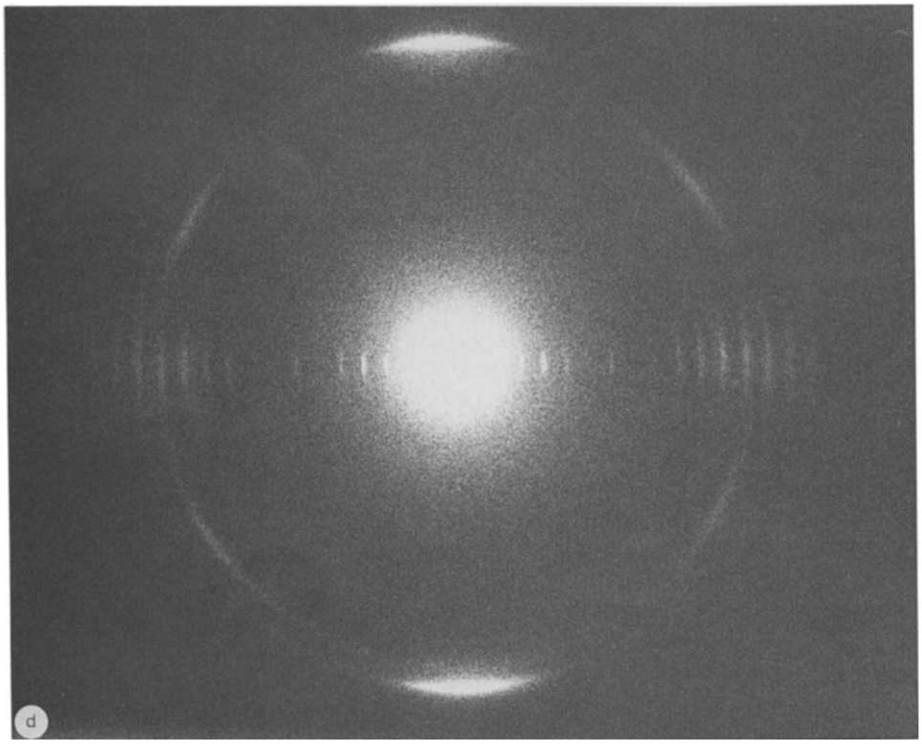

Fig. 3 continued.

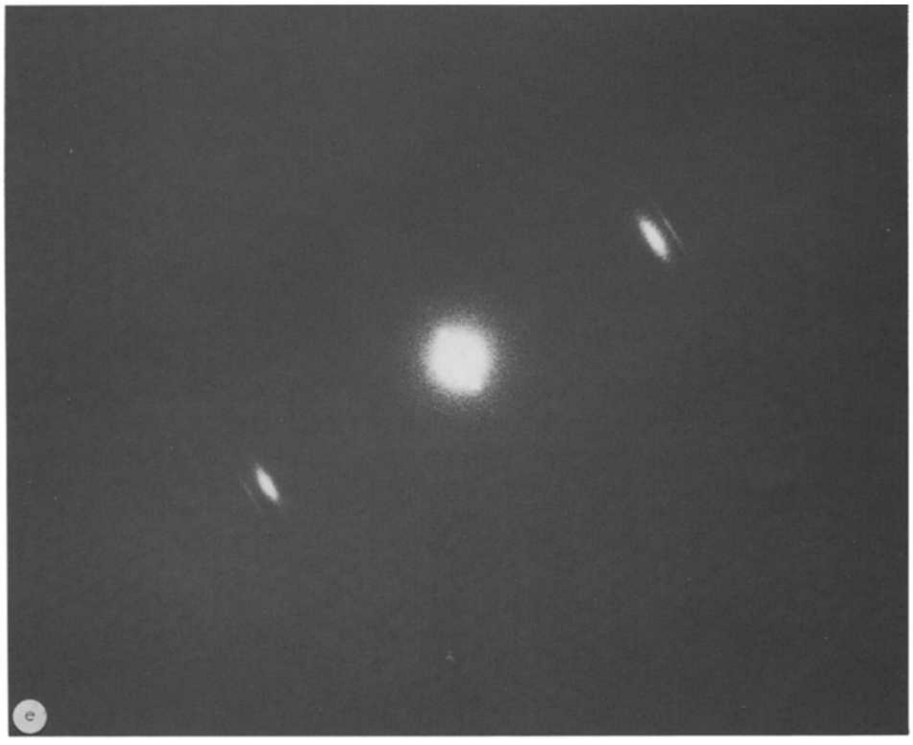

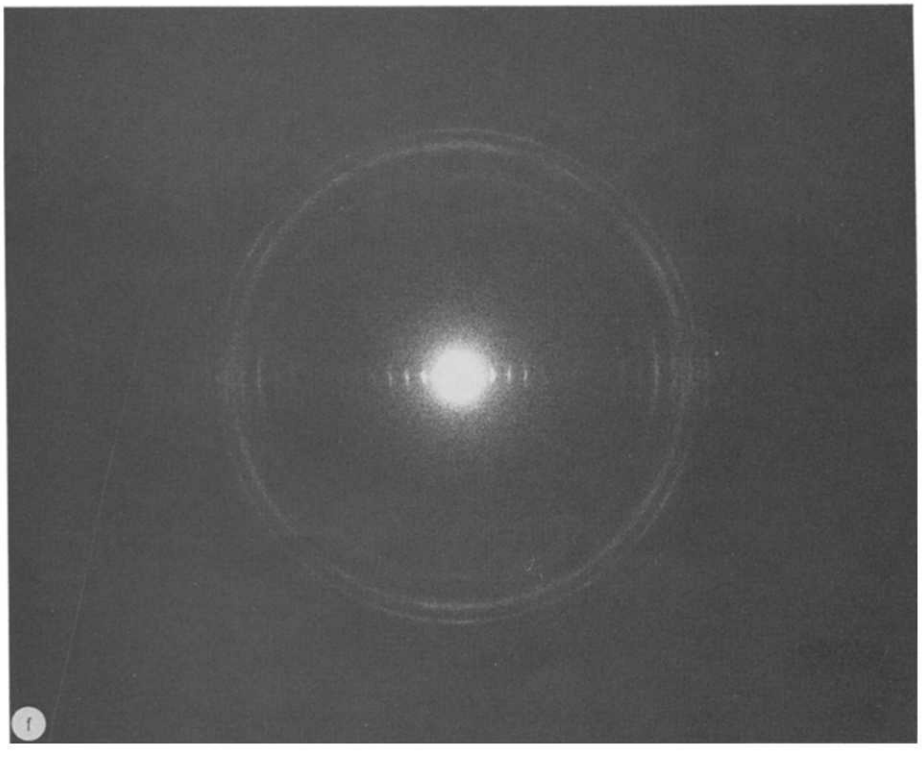

Fig. 3 continued.

from the anhydrous phospholipid crystals at various temperatures are compared in Fig. 3 including one from the liquid crystalline phase. Lattice images from the epitaxially-grown crystalline phase (Fig. 4a) reveal the curvilinear nature of the lamellae, which is a type of paracrystalline packing, as shown earlier [39].

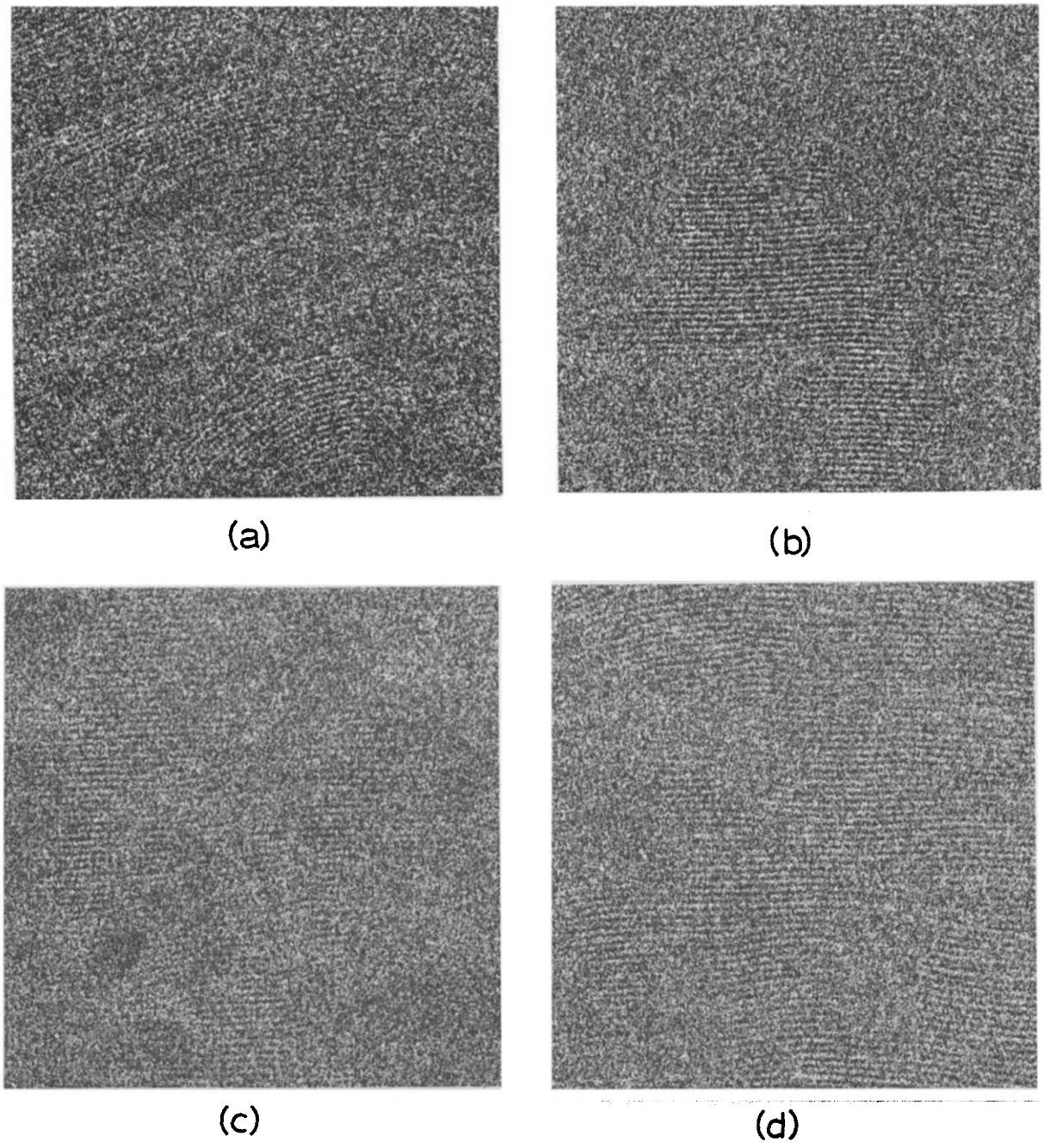

Fig. 4. Low-dose structure images from binary solid solutions of DLPE/DPPE (a) 1:0, (b) 4:1, (c) 3:1, (d) 2:1, (e) 1:1, (f) 1:2, (g) 1:3, (h) 1:4. Note characteristic curvilinear distortions of the lamellae. Optical transforms of such images were used to construct the lamellar spacing vs. composition curves in Fig. 7b.

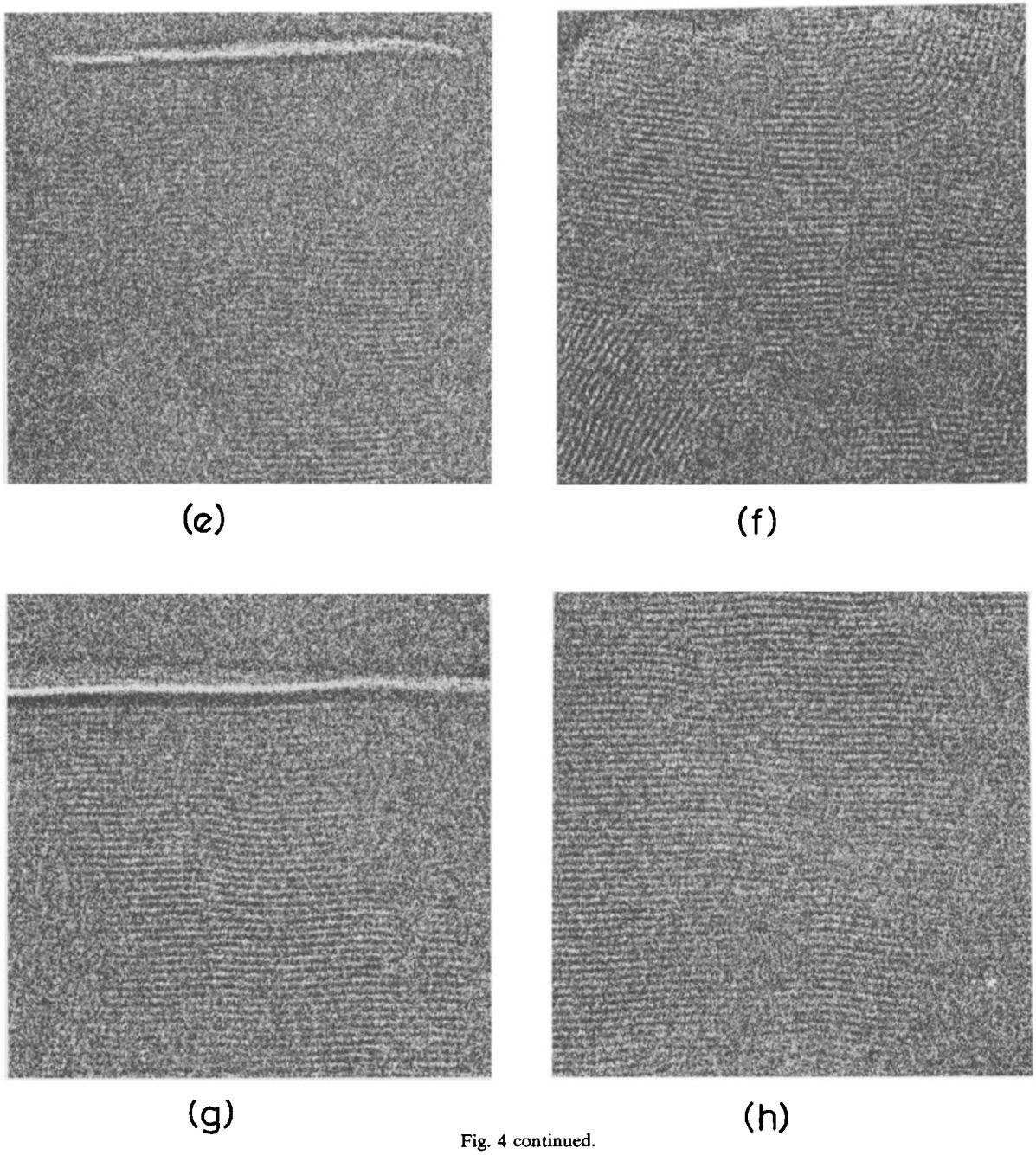

Fig. 4 continued.

Phase behavior of binary phosphatidylethanolamine mixtures

In the co-miscibility study, two variables which may influence the formation of solid solutions are studied, while keeping the nature of the headgroup interactions constant. The major influence on the relative molecular volumes is the relative chain lengths of the two lipid components and a minor influence may be due to the substitution of an ether-linkage of chains to the glycerol moiety for

TABLE I

CRYSTALLINE TO SMECTIC PHASE TRANSITIONS FOR ANHYDROUS PHOSPHATIDYLETHANOLAMINES OBTAINED FROM DIFFRACTION MEASUREMENTS ON HEATED SAMPLES

e.d., electron diffraction.

Compound	T (°C)	Measurement	DSC onset-return (°C)
1,2-Dimyristoyl-*sn*-glycerophosphoethanolamine (L-DMPE)	approx. 100	e.d.	88.0 → 101.5
1,2-Dimyristoyl-*rac*-glycerophosphoethanolamine (DL-DMPE)	112–116	X-ray [49]	–
1,2-Dihexadecyl-*sn*-glycerophosphoethanolamine (L-DHPE)	approx. 100	e.d.	92.9 → 102.7
1,2-Dipalmitoyl-*sn*-glycerophosphoethanolamine (L-DPPE)	100	e.d.	90.0 → 108.6
1,2-Dipalmitoyl-*rac*-glycerophosphoethanolamine (DL-DPPE)	111 (epitaxial)	e.d.	118.6 → 126.3
	> 121 (solution grown)		

the normal ester-linkage. The continuity of the binary systems is assessed by phase diagrams drawn from DSC scans of mixtures solidified by solvent evaporation, and by plots of lamellar spacing vs. composition found from electron diffraction patterns at different compositions and/or from optical transforms of low-dose lattice images. Results from four different studies are reviewed in the following.

DLPE/DMPE. DSC scans of different mole ratios of the chiral dilauroyl- and dimyristoylphosphatidylethanolamines contain two endo-

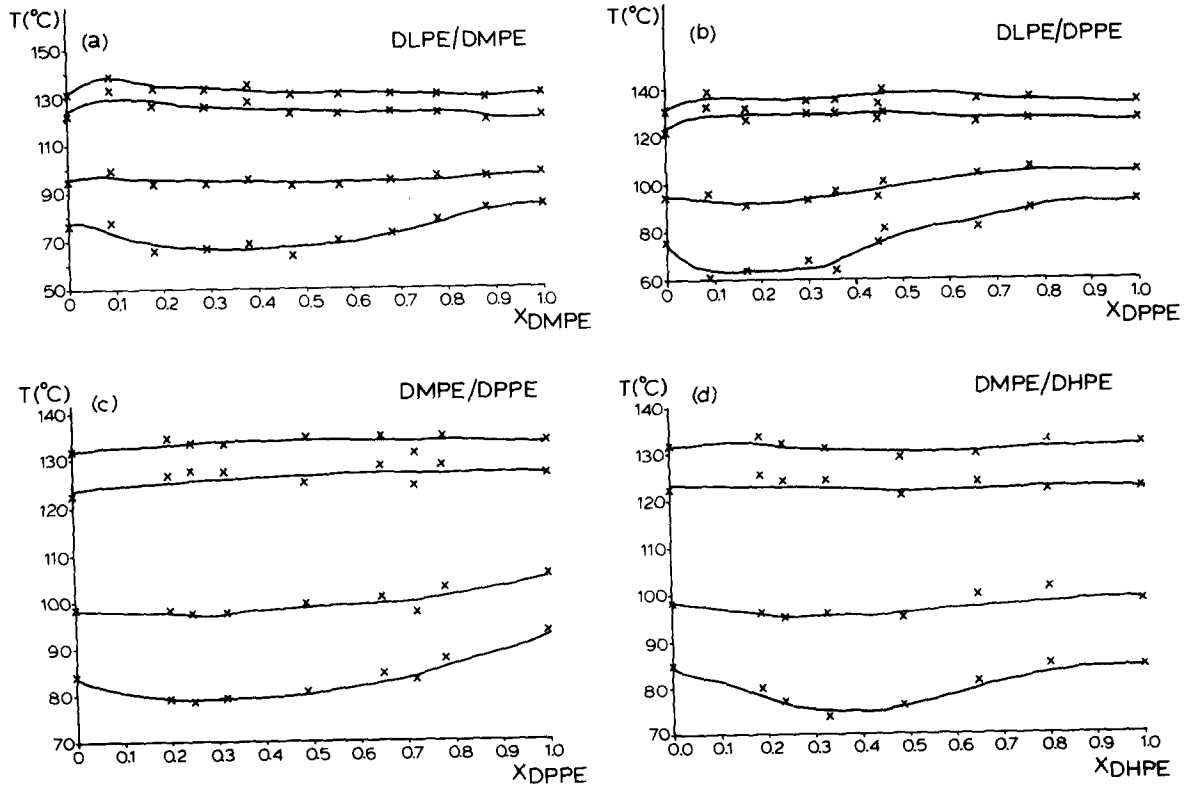

Fig. 5. Phase diagrams of various chiral phosphatidylethanolamine binary mixtures: (a) DLPE/DPPE, (b) DLPE/DPPE, (c) DMPE/DPPE, (d) DMPE/DHPE. These diagrams are constructed from onset and return temperatures of DSC endotherms similar to those shown in Fig. 1.

thermic transitions similar to those seen for pure components (Fig. 1). The low temperature endotherms for intermediate mixtures sometimes have a shoulder but, although the onset temperature may be nearly isothermal for successive concentration values in the phase diagram (Fig. 5a), no clear evidence is found for fractionation, although the continuous solubility appears to be non-ideal, as also found for some hydrated binary fractions of phosphatidylcholines [18,19,21]. Electron diffraction data from epitaxially crystallized specimens appear to indicate a bimodal distribution of lamellar spacings (Fig. 6a) but optical transforms of structure images show that intermediate concentrations are close to the lamellar specings predicted by Vegard's law (Fig. 7a).

DLPE/DPPE. Calorimeter scans at a larger chain length difference are not greatly different

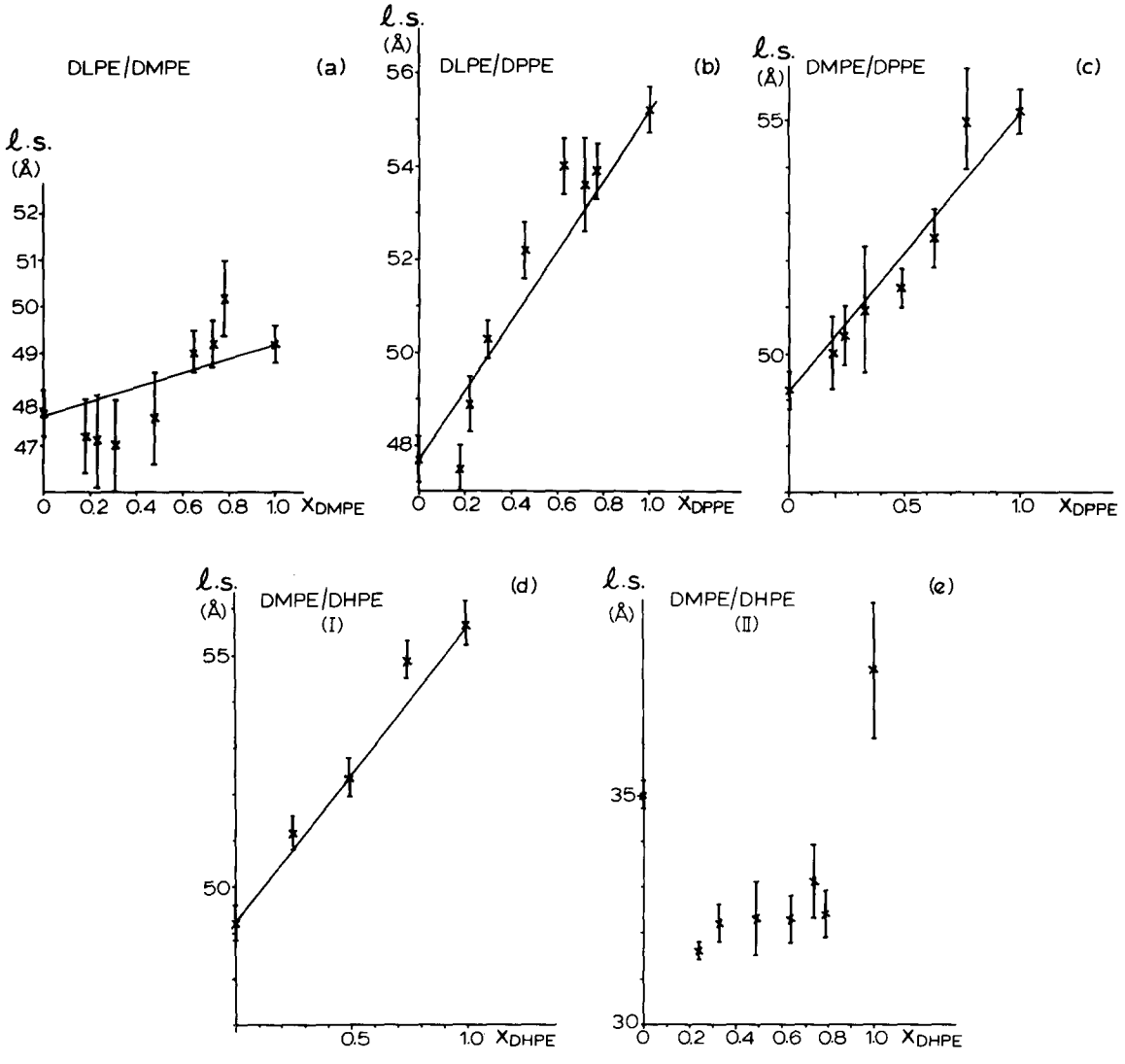

Fig. 6. Determinations of lamellar spacing from electron diffraction patterns from various binary mixtures of chiral phosphatidylethanolamines: (a) DLPE/DMPE, (b) DLPE/DPPE, (c) DMPE/DPPE, (d) DMPE/DHPE. These spacings all represent the crystalline phase and the Vegard's law line [50] connects the lamellar spacings of the pure components. Lamellar spacings have also been recorded from the smectic mesophase (e) but the values are seen to be smaller than those obtained by thermotropic phase transition of the pure components.

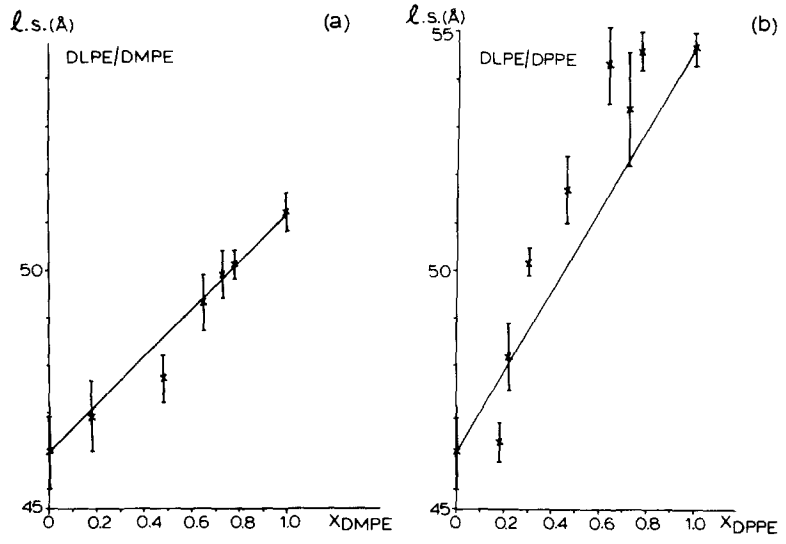

Fig. 7. Lamellar spacings of various binary mixtures determined from optical transforms of experimental structure images (e.g. Fig. 4): (a) DLPE/DMPE, (b) DLPE/DPPE; the Vegard's law line is drawn as in Fig. 6.

from the previous example. The presence of partially split crystal to smectic endotherm peaks is found less often than in the previous example. Although a small isothermal onset region may be indicated in the phase diagram (Fig. 5b), a plot of lamellar spacing vs. composition either from electron diffraction patterns (Fig. 6b) or optical transforms of structure images (Fig. 7b) indicates that the intermediate mole ratios are continuous. The latter plot in particular reveals that a measureable excess volume may be found for some fractions containing a large amount of the pure longer chain component. Representative structure images are shown in Fig. 4.

DMPE / DPPE. Endotherms in calorimeter scans for DMPE/DPPE binary solids again resemble Fig. 1 except that these are single peaks for all mole fractions. Both the phase diagram (Fig. 5c) and the lamellar spacing vs. composition curve (obtained from electron diffraction measurements) (Fig. 6c) indicate continuity of the solid solution. Occasionally, lamellar spacings due to the liquid crystal phase were also seen in electron diffraction patterns.

DMPE / DHPE. Substitution of an ester linkage by an ether linkage in one of the components does not change the phase diagram very much (compare Fig. 5d to Fig. 5c). Lamellar spacings from electron diffraction pattern of the binary crystals (Fig. 6d) are again close to the Vegard's law line. For this lipid mixture, diffraction patterns from a structure with a shorter lamellar spacing (Fig. 6e) are also commonly observed. The spacings, however, are somewhat shorter than those found for the liquid crystalline phase of the pure components produced in heating experiments (Fig. 6e).

Discussion

In a previous paper, the similarity of crystal packings for optically active an racemic phosphatidylethanolamine was established by electron diffraction structure analysis [34], a feature also demonstrated in a recent X-ray analysis [35]. Data presented in Table I, on the other hand, indicate the racemic mixture may be more stable than the chiral lipid packing, since the melting points of analogous racemic mixtures are always higher than that of the non-centrosymmetric structure. This observation is opposite to the finding for phosphatidylcholines for which addition of the oppositely-handed molecule disrupts a low temperature crystal form, as evidenced by the disappearance of a calorimetric endotherm [44].

Within a given headgroup packing, the rules for miscibility in anhydrous phosphatidylethanolamines seem to be similar to the fully hydrated phosphatidylcholines [18–21] and phosphatidyl-

ethanolamines [22]. It is clear that a chain length difference of two methylene groups per acyl chain permits the formation of continuous solid solutions and that the volume and/or conformational change caused by substitution of an ether linkage for an ester linkage also is not sufficient to cause fractionation. Increase of chain length difference by four methylene groups was anticipated to induce molecular fractionation by analogy to the extensive work on phosphatidylcholines [18–21] (data which, nevertheless, are variously interpreted). This is not the case for the phosphatidylethanolamines, however, as indicated by the data in Figs. 5, 6 and 7. Nevertheless the occurrence of isothermal segments for the onset temperatures in the phase diagram of Fig. 5 indicate that the molecular cosolubility, although continuous, is also non-ideal.

In most cases, the average lamellar spacings measured from electron diffraction patterns or optical transfocus of electron microscope images (Figs. 6, 7) lie near or above the Vegard's law line, indicating, respectively, a continuous change in unit cell volume with increasing mole fraction of higher molecular weight component or the presence of an excess volume which, for paraffins, has been ascribed to voids at the chain end boundaries [45–47]. The anomalous behavior in the DLPE/DMPE binary solids, as indicated by the electron diffraction lamellar spacings in Fig. 6a, is not understood. It may indicate a poor mixing of components occurred with the solution of two lipids was evaporated to dryness. The lamellar spacings determined from electron micrographs actually represent much smaller areas than used for selected area electron diffraction (e.g. 0.5 μm vs. 10 μm diameter) and the continuous areas in Fig. 7a may represent smaller areas where the co-solubility is more complete. Alternatively the differences between Figs. 6a and 7a may merely express a statistical variation for a relatively small number of samples used to form an average. (It is a well known weakness of electron microscope measurements that unbiased 'bulk' averages over a distribution of microstates may be difficult to obtain. The study of individual binary microcrystals, on the other hand, can lead to clues about preferred structural aggregations which are not evident from bulk measurements, as will be shown in a future publication on binary paraffin solid solutions.) A general conclusion which can be drawn from the calorimetric and diffraction data is that the rules for solid solution formation appear to conform to those proposed originally by Kitaigorodskii [27]. First, the crystal structures of the pure components in the binary solids are similar enough (indeed identical in this case [34]) to permit comiscibility with no increase of the overall symmetry. Secondly, the molecular volumes are similar enough that the free energy of the solid solution can be lower that that of either of the pure components. Just how a chain length difference of four carbons can be accommodated in a solid solution must be reserved for future consideration.

A curious feature seen in the lamellar spacing plots in Fig. 6 is the large difference in layer thickness between the putative interdigitated structure in the smectic state seen for heated pure lipids (e.g. Fig. 3c) and the one found for the higher energy forms of the binary solid solutions (e.g. Fig. 3e). A partial explanation for this might be postulated from a comparison of structure analyses for the interdigitated form of hydrated 1,2-dihexadecyl-*sn*-glycerophosphocholine [43] and the crystal structure of 1,2-dilauroyl-*rac*-glycerophospho-*N*,*N*-dimethylethanolamine [5]. The former packs with interdigitated polymethylene chains and the latter with interdigitating head groups, both forming a lamellar layer which is smaller than the usual bilayer; the interdigitated chain structure has the smallest lamellar spacing. That an interdigitated chain packing is also possible for an anhydrous lipid crystal structure has been found recently in a quantitative structure analysis of a polymorph of 1,2-dihexadecyl-*sn*-glycerophospho-*N*-methylethanolamine (Dorset, D.L., unpublished data).

Finally it is gratifying that electron diffraction data from binary phospholipid solid solutions can be obtained at sufficient resolution for future quantitative structure analyses (e.g. Figs. 3d and 3f). With the recent development of techniques for determination of crystal structures from such data [34,48] it is hoped that a more complete analysis of the molecular packing might be as successful as the one completed already for a paraffin solid solution [29].

Acknowledgements

Research was supported by a grant from the Manufacturers and Traders Trust Company for which the authors express their gratitude.

References

1 Hitchcock, P.B., Mason, R., Thomas, K.M. and Shipley, G.G. (1974) Proc. Natl. Acad. Sci. U.S.A. 71, 3036–3040
2 Elder, M., Hitchcock, P., Mason, R. and Shipley, G.G. (1977) Proc. Roy. Soc. (London) A354, 157–170
3 Pearson, R.H. and Pascher, I. (1979) Nature 281, 499–501
4 Harlos, K., Eibl, H., Pascher, I. and Sundell, S. (1984) Chem. Phys. Lipids 34, 115–126
5 Pascher, I. and Sundell, S. (1986) Biochim. Biophys. Acta 855, 68–78
6 Büldt, G., Gally, U., Seelig, J. and Zaccai, G. (1979) J. Mol. Biol. 134, 673–691
7 Zaccai, G., Büldt, G., Seelig, A. and Seelig, J. (1979) J. Mol. Biol. 134, 693–706
8 Büldt, G. and Seelig, J. (1980) Biochemistry 19, 6170–6175
9 Caspar, D.L.D. and Kirschner, D.A. (1971) Nature New Biol. 231, 46–52
10 Worthington, C.R. and McIntosh, T.J. (1973) Nature New Biol. 245, 97–99
11 Harker, D. (1972) Biophys. J. 12, 1285–1295
12 King, G.I. (1975) Acta Cryst. A31, 130–135
13 Levine, Y.K. (1973) Progr. Surf. Sci. 3, 279–352
14 Torbet, J. and Wilkins, M.H.F. (1976) J. Theoret Biol. 62, 447–458
15 Khare, R.S. and Worthington, C.R. (1978) Biochim. Biophys. Acta 514, 239–254
16 McIntosh, T.J. (1980) Biophys. J. 29, 237–245
17 McIntosh, T.J., Simon, S.A., Ellington, J.C., Jr. and Porter, N.A. (1984) Biochemistry 23, 4038–4044
18 Lee, A.G. (1978) Biochim. Biophys. Acta 507, 433–444
19 Mabrey, S. and Sturtevant, J.M. (1976) Proc. Natl. Acad. Sci. U.S.A. 73, 3862–3866
20 Phillips, M.C., Ladbrooke, B.D. and Chapman, D. (1970) Biochim. Biophys. Acta 196, 35–44
21 Van Dijck, P.W.M., Kaper, A.J., Oonk, H.A.J. and De Gier, J. (1974) Biochim. Biophys. Acta 470, 58–69
22 Dörfler, H.-D. and Brezesinski, G. (1983) Colloid Polym. Sci. 261, 427–433
23 Dörfler, H.-D. and Brezesinski, G. (1983) Colloid Polym. Sci. 261, 245–250
24 Dörfler, H.-D., Diele, S. and Diehl, M. (1984) Colloid Polym. Sci. 262, 131–138
25 Dörfler, H.-D., Diele, S. and Diehl, M. (1984) Colloid Polym. Sci. 262, 139–145
26 Finegold, L., Melnick, S.J. and Singer, M.A. (1985) Chem. Phys. Lipids 38, 387–390
27 Kitaigorodskii, A.I. (1961) Organic Chemical Crystallography, pp. 231, 2450, Consultants Bureau, New York
28 Albon, N. (1976) J. Cryst. Growth 35, 105–109
29 Dorset, D.L. (1985) Macromolecules 18, 2158–2163
30 Dorset, D.L. (1986) Macromolecules, 19, 2965–2973
31 Dorset, D.L. (1987) J. Lipid Res., in the press
32 Green, J.P., Phillips, M.C. and Shipley, G.G. (1973) Biochim. Biophys. Acta 330, 243–253
33 Hitchcock, P.B., Mason, R. and Shipley, G.G. (1975) J. Mol. Biol. 94, 297–299
34 Dorset, D.L., Massalski, A.K. and Fryer, J.R. (1987) Z. Naturforsch. 42a, 381–391
35 Suwalsky, M. and Duk, L. (1987) Makromol. Chem. 188, 599–606
36 Blume, A., Arnold, B. and Weltzien, H.U. (1976) FEBS Lett. 61, 199–202
37 Wittmann, J.C. and Lotz, B. (1985) Inst. Phys. Conf. Ser. 78, 417–422
38 Dorset, D.L. (1985) J. Electron Microsc. Techn. 2, 89–128
39 Fryer, J.R. and Dorset, D.L. (1987) J. Microsc. (Oxford) 145, 61–68
40 Chapman, D., Byrne, P. and Shipley, G.G. (1966) Proc. Roy. Soc. (London) A290, 115–142
41 McIntosh, T.J., McDaniel, R.V. and Simon, S.A. (1983) Biochim. Biophys. Acta 731, 109–114
42 Hui, S.W., Mason, J.T. and Huang, C.-H. (1984) Biochemistry 23, 5570–5577
43 Ruocco, M.J., Siminovitch, D.J. and Griffin, R.G. (1985) Biochemistry 24, 2406–2411
44 Boyanov, A.I., Koynova, R.D. and Tenchov, B.G. (1986) Chem. Phys. Lipids 39, 155–163
45 Mnyukh, Yu.V. (1959) Zh. Strukt. Khim. 1, 370–388
46 Asbach, G.I., Kilian, H.G. and Stracke, Fr. (1982) Colloid Polym. Sci. 260, 151–163
47 Craievich, A., Doucet, J. and Denicolo, I. (1984) J. Phys. 45, 1473–1477
48 Dorset, D.L. (1987) Biochim. Biophys. Acta 898, 121–128
49 Williams, R.M. and Chapman, D. (1971) Progr. Chem. Fats Other Lipids 11, 1–79
50 Kitaigorodsky, A.I. (1984) Mixed Crystals, p. 167, Springer Verlag, Berlin